Journal of Applied Polymer Science

# Synthesis, characterization, and curing behavior of carborane-containing benzoxazine resins with excellent thermal and thermo-oxidative stability

**Shicheng Qi, Hongrui Wang, Guo Han, Zhen Yang, Xiao A Zhang, Shengling Jiang, Yafei Lu**
Key Laboratory of Carbon Fiber and Functional Polymers of Ministry of Education, College of Materials Science and Engineering, Beijing University of Chemical Technology, Beijing 100029, China
Correspondence to: X. A. Zhang (E-mail: zhangxiaoa1982@163.com)

**ABSTRACT:** Two benzoxazine precursors bearing carborane moiety (**1** and **2**) were designed and synthesized successfully by the Mannich reaction of corresponding carborane bisphenol (**3** and **4**) with aniline and formaldehyde in 1,4-dioxane. The obtained precursors were characterized by using multiple spectroscopic techniques including GPC, FTIR, $^{1}$H NMR, $^{13}$C NMR, and $^{11}$B NMR. Nonisothermal DSC studies showed that precursor **1** owned lower apparent activation energies ($E_a$) than **2**. The optimum curing processes of benzoxazine precursors were also obtained on the basis of DSC data. TGA analyses manifested that the incorporation of carborane moiety endowed the obtained benzoxazine resins (cured **1** and **2**) with excellent thermal stability and unique thermo-oxidative stability. The $T_d$ data showed that the initial degradation of both cured **1** and **2** under nitrogen and air was postponed to some extent owing to the shielding effect of carborane moiety on adjacent organic fragments. At higher temperature three-dimensional polymer networks with B-O-B and B–C linkages were formed as chars by the reaction of carborane cage with atmospheric moisture, degradation products such as phenolic hydroxyl, and oxygen (under air). Under nitrogen this network hindered the motion of radicals formed at elevated temperature and thus inhibited further polymer degradation processes. While under air, the formed boron-rich networks could hardly be further oxidized into carbon dioxide so that the carborane-containing benzoxazine resins also showed very high char yields. © 2016 Wiley Periodicals, Inc. J. Appl. Polym. Sci. **2016**, *133*, 43488.

**KEYWORDS:** resins; thermogravimetric analysis; thermal properties; thermosets

Received 13 October 2015; accepted 1 February 2016
**DOI: 10.1002/app.43488**

## INTRODUCTION

As a new type of addition-curable phenolic resin, benzoxazine resins have exhibited many superior performances such as high thermal stability, no evolution of volatiles and near-zero shrinkage during curing, flexibility of molecular design, and tailored mechanical properties.[1] They could be utilized to prepare various materials such as high-performance adhesives and fiber-reinforced composites.[2] However, benzoxazine resins possess low density and are rather brittle, which limits their application.[3] Furthermore, benzoxazine resins are increasingly required to own higher properties such as thermal stability in high-tech fields. On one hand, to obtain higher thermal stability, benzoxazine resins were incorporated with addition reaction groups such as acetenyl,[4,5] allyl,[6,7] cyano,[8,9] maleimide,[10,11] and furan[12] which could participate in the curing reaction and thus improved the degree of curing. On the other hand, bulky moieties such as fluorenyl,[13,14] adamantine,[15] and naphthalene[16] were also introduced to the molecular structure of benzoxazine resins so as to enhance their heat resistance. To date the search for new high-temperature units is still attracting much attention.

*Closo*-carboranes ($C_2B_{10}H_{12}$), with an icosahedral geometry, are excellent building blocks for thermally stable polymers.[17] Carboranes could absorb energy like a kind of "power gauge" at high temperature owing to its "superaromatic" electronic structure. Besides, the large volume of three-dimensional cage endows carboranes with strong shielding effect on adjacent segments. Therefore, carboranes were incorporated into many traditional polymers to improve their thermal stability including polysiloxanes,[18–26] epoxy resins,[27,28] phenolic resins,[29,30] aromatic polymers,[31] etc. With the increasing appearance of new polymers, carboranes expanded their application fields such as dendrimers[32–38] and conjugated polymers with light-emission property.[39–44]

Additional Supporting Information may be found in the online version of this article.

By virtue of the flexibility of molecular design, benzoxazine resins have been synthesized from various bisphenol, such as bisphenol A,[45–47] bisphenol S,[48,49] bisphenol AP,[50] and bisphenol fluorenyl.[51,52] We have successfully synthesized carborane bisphenols and corresponding carborane-based epoxy resins[28] and phenolic resins.[30] Although carborane bisphenols have been proved to be excellent starting materials for many carborane-containing polymers, to the best of our knowledge, they have not been utilized to synthesize benzoxazine polymers. Jia *et al.*[53] synthesized main-chain polybenzoxazine with *m*-carborane on its backbone by click polymerization of alkyne-containing benzoxazine and azido-substituted *m*-carborane. In this work, we report our studies on carborane-containing benzoxazine resins from carborane bisphenols. Two carborane bisphenol benzoxazine precursors (**1** and **2**) were synthesized by Mannich reaction of carborane bisphenol, formaldehyde, and aniline. Their chemical structures have been well characterized, and their curing behaviors and thermal and thermo-oxidative stability were studied.

## EXPERIMENTAL

### Materials

*o*(*m*)-carborane bisphenol was synthesized and purified according to our previously published synthetic route.[30] Aniline was obtained from Tianjin recovery technology development. Formaldehyde aqueous solution (37 wt %) was provided by Xilong Chemical. 1,4-dioxane, Chloroform and sodium hydroxide were purchased from Beijing Chemical Factory (Beijing, China). All the chemicals were used as received without any further purification.

### Instrumentation

FTIR spectra were recorded in the range of 4000–400 $cm^{-1}$ on a Nexus 670 FTIR spectrophotometer and the samples were finely ground with KBr powder and pressed into disk. $^{1}H$, $^{13}C$, and $^{11}B$ NMR spectra were acquired in deuterated chloroform on a Bruker AV400 at a proton frequency of 400 MHz and the corresponding carbon and boron frequencies. Tetramethylsilane was used as an internal standard. Molecular weight ($M_n$) and polydispersity indices ($M_w/M_n$) of the precursors were tested in THF with a Waters 515 gel permeation chromatography system. Nonisothermal differential scanning calorimetric measurements were conducted using a TA Q1000 DSC operating in a nitrogen atmosphere and the heating rate was set as 5, 10, 15, and 20 °C/min respectively, heated from 30 to 300 °C. The TGA analysis was performed on a TA SDT-Q600 thermogravimetric analyzer at a heating rate of 20 °C/min from 50 to 900 °C under nitrogen and air atmosphere.

### Synthesis of Carborane Bisphenol Benzoxazine Precursors (1 and 2)

Carborane bisphenol benzoxazine precursors (**1** and **2**) were synthesized according to the synthetic routes shown in Scheme 1. The detailed procedures for the synthesis of **2** were given below as an example.

Formaldehyde aqueous solution (37 wt %, 0.3245 g, 0.004 mol) and 1,4-dioxane (8 mL) were added to a 100 mL three-necked round bottom flask equipped with a magnetic stirrer, a thermometer, and a reflux condensing tube. After the mixture was cooled below 10 °C in an ice bath, aniline (0.1862 g, 0.002 mol) in 1,4-dioxane (2 mL) was added dropwise to the flask. The mixture was magnetically stirred for 30 min and then *m*-carborane bisphenol (**4**, 0.3282 g, 0.001 mol) in 1,4-dioxane (10 mL) was added. The temperature was then raised to 94 °C and the mixture was stirred for 8 h. After cooling to room temperature, the solvent was removed by rotary evaporation. The obtained viscous fluid was then dissolved in 80 mL chloroform and washed three times with 1.5 mol/L NaOH solution and deionized water, respectively. The chloroform was evaporated by rotary evaporation and the resultant product was dried in a vacuum oven overnight. A pale yellow solid was obtained in a yield of 89.2%. $M_n$: 512; $M_w/M_n$: 1.26 (GPC, polystyrene calibration; Table II, No. 2). FTIR, $\nu$ ($cm^{-1}$, in KBr pellet): 3064, 3036 (=C—H), 2940, 2846 (C—H), 2600 (B—H), 1598, 1499, 1455, 1385 and 1162 (C—N—C), 1228 and 1034 (C—O—C), 971 (oxazine ring), 838, 751. $^{1}H$ NMR (400 MHz, $CDCl_3$), $\delta$ (TMS, ppm): 7.30–6.70 (m, aromatic protons), 5.34 (s, O—$CH_2$—N), 4.61 (s, Ar—$CH_2$—N), 3.80 (s, Ar—$CH_2$—NH), 3.20–1.20 (m, B—H). $^{13}C$ NMR (100 MHz, $CDCl_3$), $\delta$ (TMS, ppm): 163.3–113.4 (aromatic carbons), 79.6 (O—$CH_2$—N), 78.3 (C of carborane), 50.7 (Ar—$CH_2$—N). $^{11}B$ NMR (128 MHz, $CDCl_3$), $\delta$ (TMS, ppm): −6.45, −10.68, −13.44.

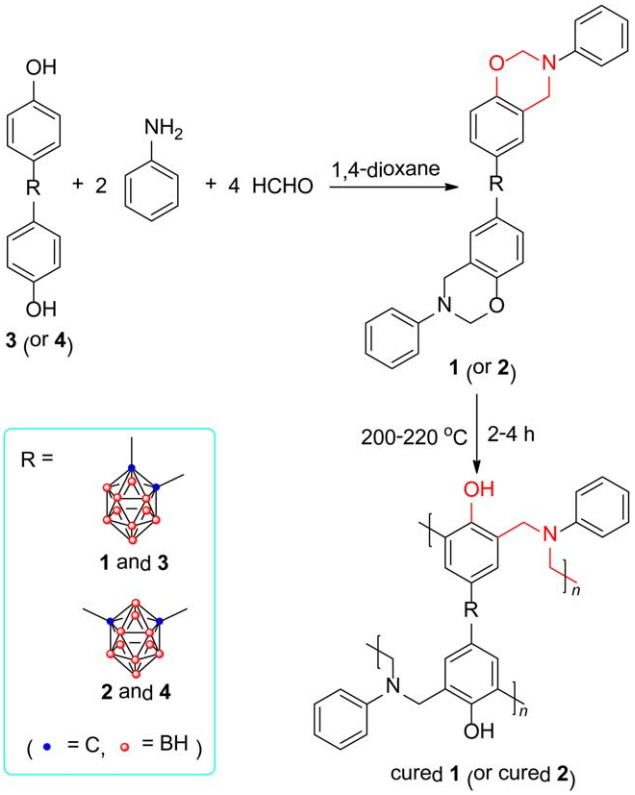


**Scheme 1.** Synthesis and curing of carborane bisphenol benzoxazine precursors (**1** and **2**). [Color figure can be viewed in the online issue, which is available at wileyonlinelibrary.com.]

Characterization data for **1**: pale yellow solid, 85.1%. $M_n$: 431; $M_w/M_n$: 1.35 (GPC, polystyrene calibration; Table I, No. 2). FTIR, $\nu$ ($cm^{-1}$, in KBr pellet): 3065, 3036 (=C—H), 2941, 2846

**Table I.** The Synthesis of *o*-Carborane Bisphenol Benzoxazine Precursor (1)[a]

| No. | *T*, °C | *t*, h | yield, % | $M_n$[b] | $M_w/M_n$[b] | Ring content[c], % |
|---|---|---|---|---|---|---|
| 1 | 94 | 8 | 82.0 | 290 | 1.20 | 26.0 |
| 2 | 94 | 10 | 85.1 | 431 | 1.35 | 69.5 |
| 3 | 94 | 12 | 84.2 | 346 | 1.29 | 39.4 |
| 4 | 88 | 10 | 81.8 | 293 | 1.25 | 12.4 |
| 5 | 100 | 10 | 82.3 | 404 | 1.28 | 67.4 |

[a] Carried out in 1,4-dioxane, $[o\text{-carborane bisphenol}]_0$: $[\text{anline}]_0$: $[\text{formaldehyde}]_0 = 1:2:4$.
[b] Estimated by gel permeation chromatograph (GPC) in THF on the basis of polystyrene calibration.
[c] Calculated from NMR data,[54] see "Structure Characterization of Carborane Bisphenol Benzoxazine Precursors (1 and 2)" for detail.

(C—H), 2583 (B—H), 1598, 1499, 1456, 1385, and 1162 (C—N—C), 1228 and 1034 (C—O—C), 971 (oxazine ring), 838, 751. $^1$H NMR (400 MHz, $CDCl_3$), $\delta$ (TMS, ppm): 7.30–6.40 (m, aromatic protons), 5.16 (s, O—$CH_2$—N), 4.30 (s, Ar—$CH_2$—N), 3.61 (s, Ar—$CH_2$—NH), 3.20–1.20 (m, B—H). $^{13}$C NMR (100 MHz, $CDCl_3$), $\delta$ (TMS, ppm): 162.1–111.8 (aromatic carbons), 84.6 (carbons on carborane cage), 79.0 (O—$CH_2$—N), 49.0 (Ar—$CH_2$—N). $^{11}$B NMR (128 MHz, $CDCl_3$), $\delta$ (TMS, ppm): −2.92, −9.52, −10.94.

### Curing of Carborane Bisphenol Benzoxazine Precursors (1 and 2)

Carborane bisphenol benzoxazine precursors (**1** and **2**) were cured without the curing agent according to a temperature-programmed process (200 °C/2 h + 220 °C/2 h for precursor **1** and 150 °C/2 h + 240 °C/2 h for precursor **2**).

Characterization data for cured **1**: reddish brown solid. FTIR, $\nu$ ($cm^{-1}$, in KBr pellet): 3356 (−OH), 3015 (unsaturated bond =C—H), 2895, 2836 (saturated bond C—H), 2600 (B—H), 1615, 1591, 1571, 1513 (benzene ring), 1385, 1162 (C—N—C) disappear, 1228, 1034 (C—O—C) disappear, 971 (oxazine ring) disappear, 812, 757 (C—H of benzene ring).

Characterization data for cured **2**: reddish brown solid. FTIR, $\nu$ ($cm^{-1}$, in KBr pellet): 3410 (—OH), 3025 (unsaturated bond =C—H), 2889 (saturated bond C—H), 2600 (B—H), 1599, 1503 (benzene ring), 1385, 1162 (C—N—C) disappear, 1228, 1034 (C—O—C) disappear, 971 (oxazine ring) disappear, 800, 751 (C—H of benzene ring).

## RESULTS AND DISCUSSION

### Synthesis of Carborane Bisphenol Benzoxazine Precursors (1 and 2)

The synthetic routes to carborane bisphenol benzoxazine precursors (**1** and **2**) are shown in Scheme 1 (the experiment details and characterization data are included in Experimental). The Mannich reaction of carborane bisphenol (**3** and **4**) with aniline and formaldehyde in 1,4-dioxane gave carborane-containing benzoxazine precursors (**1** and **2**) with expected structures. All the reactions proceeded smoothly, and the desired target precursors were isolated in satisfactory yields (~81.8–89.2%, Tables I and II).

To synthesize *o*-carborane bisphenol benzoxazine precursor (**1**) with high content of oxazine ring, 1,4-dioxane with low dielectric constant ($\varepsilon = 2.2$) was selected as reaction solvent.[1] We first attempted to conduct the reaction at 94 °C for 8 hours, and benzoxazine precursor with low $M_n$ and ring content was obtained ($M_n$ ~290, ring content ~26%, Table I, No. 1). When the reaction time was extended to 10 h, the reaction took place to such an extent that $M_n$ and ring content were increased to ~431 and 69.5% (Table I, No. 2). However, when the time was further increased to 12 h, both $M_n$ and ring content were decreased dramatically (Table I, No. 3), indicating that the formed oxazine ring was partly consumed during the reaction process. It was useless to further increase the reaction temperature for higher ring content, while lower temperature (88 °C) caused very low ring content when the reaction time was kept at 10 hours (Table I, Nos. 4–5). Therefore, it was concluded that *o*-carborane bisphenol benzoxazine precursor (**1**) with the highest ring content was obtained when the reaction was conducted at 94 °C for 10 h. Higher temperature and longer time were harmful to the ring content. The oxazine ring could hardly be broken at higher temperature in the reaction system, which may be interpreted by the strong shielding effect of *o*-carborane cage on the oxazine ring.

Similarly, *m*-carborane bisphenol benzoxazine precursor (**2**) was also synthesized in 1,4-dioxane, an apolar solvent widely used in the synthesis of benzoxazine compound.[1] The target product with the highest $M_n$ (512) and ring content (87.2%) was obtained when the reaction was conducted at 94 °C for 8 h (Table II, No. 2). It is clear that the temperature and time have the same effect on the synthesis of benzoxazine precursor **2** as **1**. Noteworthy, much lower ring content (44.6%) was obtained at higher reaction temperature (Table II, No. 5). Since *m*-carborane has weaker shielding effect than *o*-carborane on the oxazine ring, the ring was opened at high temperature and the formed methylene cation could easily attack the ortho-position of phenolic hydroxyl to produce Mannich bridge structure.

Both of the synthesized precursors (**1** and **2**) are pale yellow solid and could be solved in common organic solvents such as acetone, THF, chloroform, and DMSO. Just as bisphenol A-based benzoxazine compounds,[1] carborane-containing benzoxazine precursors could be stored and used as solid or in solution state. They could

**Table II.** The Synthesis of *m*-Carborane Bisphenol Benzoxazine Precursor (2)[a]

| No. | *T*, °C | *t*, h | yield, % | $M_n$[b] | $M_w/M_n$[b] | Ring content[c], % |
|---|---|---|---|---|---|---|
| 1 | 94 | 6 | 83.8 | 481 | 1.29 | 41.8 |
| 2 | 94 | 8 | 89.2 | 512 | 1.26 | 87.2 |
| 3 | 94 | 10 | 89.1 | 343 | 1.24 | 64.1 |
| 4 | 88 | 8 | 82.0 | 342 | 1.26 | 49.8 |
| 5 | 100 | 8 | 87.5 | 387 | 1.40 | 44.6 |

[a] Carried out in 1,4-dioxane, $[m\text{-carborane bisphenol}]_0$: $[\text{anline}]_0$: $[\text{formaldehyde}]_0 = 1:2:4$.
[b] Estimated by gel permeation chromatograph (GPC) in THF on the basis of polystyrene calibration.
[c] Calculated from NMR data,[54] see "Structure Characterization of Carborane Bisphenol Benzoxazine Precursors (1 and 2)" for detail.

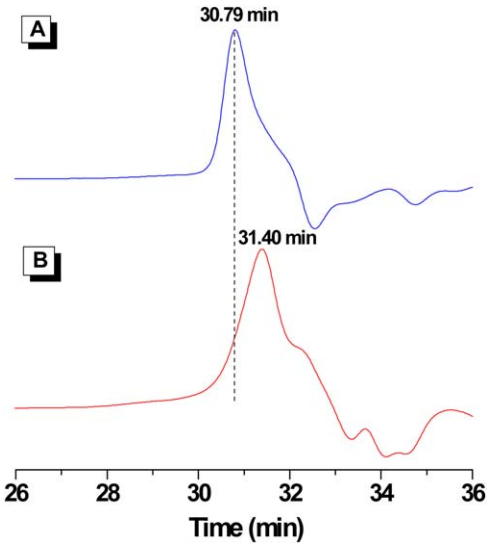


**Figure 1.** GPC chromatographs of (**A**) *m*-carborane bisphenol (**4**), and (B) *m*-carborane bisphenol benzoxazine precursor (**2**, Table II, No. 2) in THF on the basis of polystyrene calibration. [Color figure can be viewed in the online issue, which is available at wileyonlinelibrary.com.]

be cured by simple heating without curing agent according to a temperature-programmed process and three-dimensional cross-linked structures were obtained (Scheme 1).

### Structure Characterization of Carborane Bisphenol Benzoxazine Precursors (1 and 2)

The obtained benzoxazine precursors (**1** and **2**) were characterized with standard spectroscopic methods. Both precursors gave satisfactory analysis data corresponding to their expected molecular structures (see Experimental section for details). The structure characterization of *m*-carborane bisphenol benzoxazine precursor (**2**) was illustrated in detail below as an example. About the *o*-carborane bisphenol benzoxazine precursor (**1**), it was characterized in the supporting information.

The GPC chromatographs of precursor **2** and its corresponding bisphenol **4** are shown in Figure 1. The benzoxazine precursor **2** shows a retention time of 31.40 min, longer than its bisphenol counterpart (4) although its molecular weight is bigger. This result is illustrated by the fact that larger hydrodynamic volume will cause shorter retention time and *m*-carborane bisphenol (**4**) owns larger hydrodynamic volume due to the existence of hydroxyl groups. Besides, the single peak of the benzoxazine precursor **2** implies that the obtained precursor does not contain higher molecular weight fractions and is only composed of difunctional, monofunctional, and oxazine-free monomers (Chart 1).[54]

The FTIR spectrum of *m*-carborane bisphenol benzoxazine precursor (**2**) is shown in Figures 2 and 3; the FTIR spectrum of its starting compound **4** is also given in the same figure for comparison.[30] It is seen that **4** exhibits absorption peak at 2600 $cm^{-1}$, which is ascribed to the stretching vibration of B—H on carborane cage. This band is still present in the spectrum of **2**, indicating that the carborane cage remains intact during the synthesis of benzoxazine precursor. Besides, new

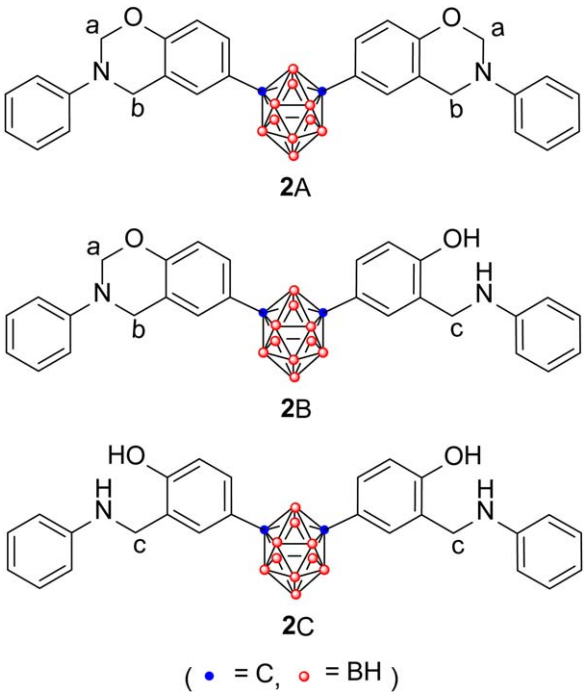


**Chart 1.** Three possible components of *m*-carborane bisphenol benzoxazine precursor (**2**). [Color figure can be viewed in the online issue, which is available at wileyonlinelibrary.com.]

peaks appear at 1034 and 1228 $cm^{-1}$ associated with the symmetric and asymmetric vibrations of C—O—C, while absorption peaks at 1162 and 1385 $cm^{-1}$ are related with the symmetric and asymmetric vibrations of C—N—C, which confirms the formation of cyclic ether of benzoxazine structure. Furthermore, wide absorption band around 3300 $cm^{-1}$ ascribe to phenolic hydroxyl group almost disappears, which is further evidence that carborane bisphenol has been transformed into benzoxazine precursor.

NMR spectroscopy is an effective method of characterizing the molecular structures. As can be seen from the $^{1}H$ NMR

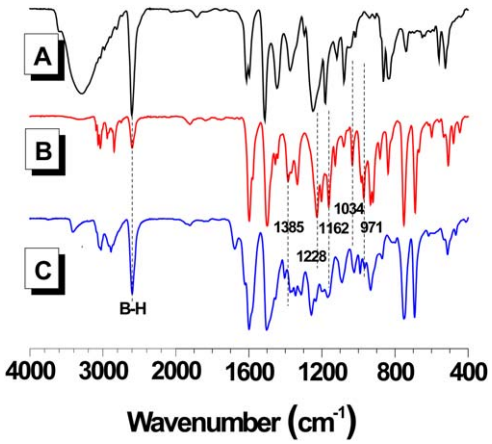


**Figure 2.** FTIR spectra of (**A**) *m*-carborane bisphenol (**4**), (B) *m*-carborane bisphenol benzoxazine precursor (**2**, Table II, No. 2), and (C) cured **2**. [Color figure can be viewed in the online issue, which is available at wileyonlinelibrary.com.]

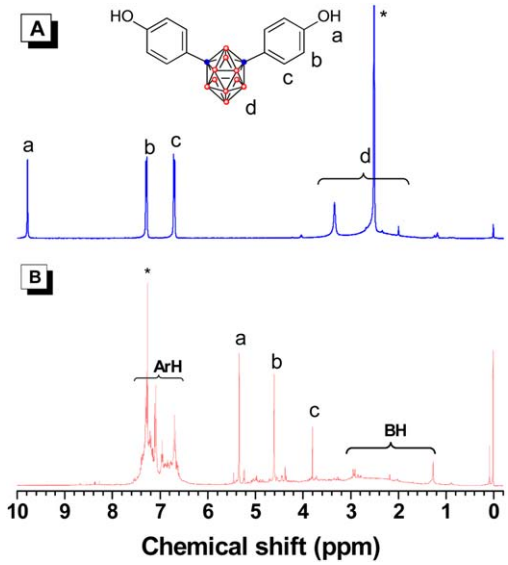


**Figure 3.** $^{1}$H NMR spectra of (**A**) *m*-carborane bisphenol (**4**) in acetone-$d_6$, and (B) *m*-carborane bisphenol benzoxazine precursor (**2**, Table II, No. 2) in $CDCl_3$. The solvent peaks are marked with asterisks. The structure of **2** is given in Chart 1. [Color figure can be viewed in the online issue, which is available at wileyonlinelibrary.com.]

spectrum of **2**, there is no resonance peak at $\delta \sim 9.79$ associated with phenolic hydroxyl group, indicating that *m*-carborane bisphenol (**4**) has been fully transformed into benzoxazine precursor **2**. New peaks appear at $\delta \sim 5.34$ and 4.61 which are attributed to the resonance of methylene protons on the oxazine ring (Chart 1, $H_a$ and $H_b$), while a resonance peak at $\delta \sim 3.80$ is related with methylene protons of the opened structure (Chart 1, $H_c$). Since the obtained precursor **2** owns three possible components and each component contains oxazine ring and/or opened structure (Chart 1), the integrated intensities of

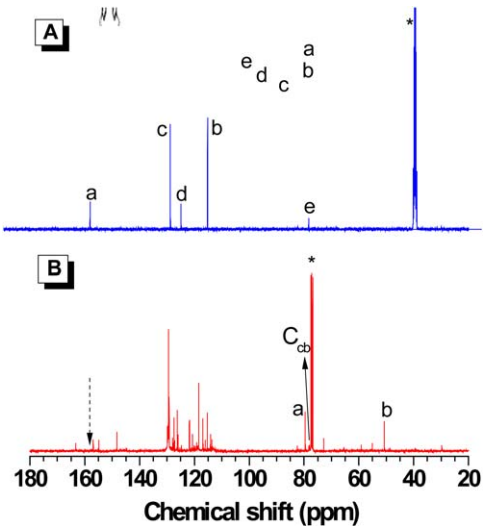


**Figure 4.** $^{13}$C NMR spectra of (**A**) *m*-carborane bisphenol (**4**) in acetone-$d_6$, and (B) *m*-carborane bisphenol benzoxazine precursor (**2**, Table II, No. 2) in $CDCl_3$. The solvent peaks are marked with asterisks. The structure of **2** is given in Chart 1. [Color figure can be viewed in the online issue, which is available at wileyonlinelibrary.com.]

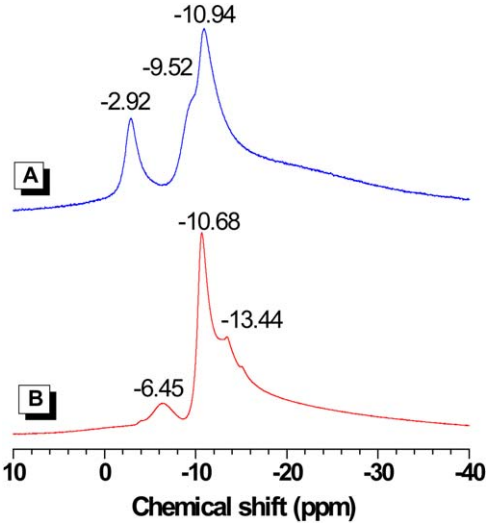


**Figure 5.** $^{11}$B NMR spectra of (**A**) *o*-carborane bisphenol benzoxazine precursor (**1**, Table I, No. 2), and (B) *m*-carborane bisphenol benzoxazine precursor (**2**, Table II, No. 2) in $CDCl_3$. [Color figure can be viewed in the online issue, which is available at wileyonlinelibrary.com.]

the above resonance peaks were utilized to calculate the percentage of benzoxazine ring, i.e. ring content, in the whole composition and the results were shown in Tables I and II.

The $^{13}$C NMR spectra of benzoxazine precursor **2** and its starting compound **4** are shown in Figure 4. It is seen that in the spectrum of **2** new peaks appear at $\delta \sim 79.6$ and 50.7 which are attributed to methylene carbons on the oxazine ring, further verifying the formation of benzoxazine precursor. Since the benzoxazine precursors (**1** and **2**) contain carborane cage, $^{11}$B NMR spectroscopy has been utilized to analyze their structures and the results are shown in Figure 5. The characteristic peaks of boron atoms of benzoxazine precursors are well consistent with their precursory carborane bisphenol.[55]

### Curing Behavior of Carborane Bisphenol Benzoxazine Precursors (1 and 2)

Nonisothermal DSC tests were utilized to study the curing kinetics of benzoxazine precursors (**1** and **2**). The nonisothermal DSC curves of *o*-carborane bisphenol benzoxazine precursor (**1**) and *m*-carborane bisphenol benzoxazine precursor (**2**) at different heating rates were given in Figures 6 and 7. It is clear that exothermic peaks shift to higher temperatures with the increase of heating rate, which is consistent with the typical curing behavior of thermosetting resins.[52] As the temperature increases, the molecules of precursor **1** and **2** absorb energy and become active. The curing reaction takes place when the activated molecules collide effectively with each other. At higher heating rate, the effective collision occurs at temperatures higher than the required minimum temperature so that the initial curing temperature shifts to higher temperature. It is worth noting that the endothermic peaks appear before the exothermic peak at the heating rate of 20 °C/min, which is probably due to the initial thermal decomposition of open ring structures of precursor **1** and **2**. Through further studying the thermal stabilities by TGA and FTIR, the open ring structures were proved to be

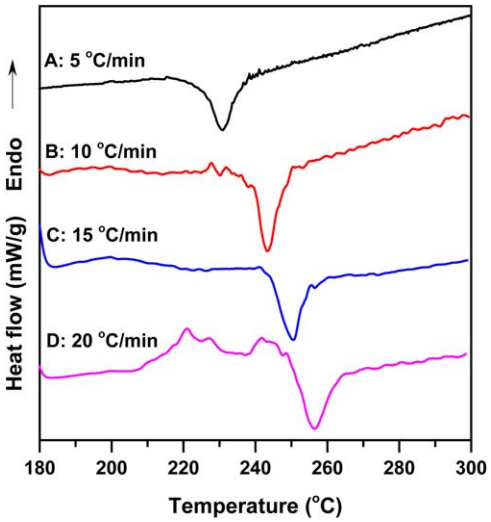


**Figure 6.** Nonisothermal DSC curves for *o*-carborane bisphenol benzoxazine precursor (**1**) at (A) 5, (B) 10, (C) 15, and (D) 20 °C/min. [Color figure can be viewed in the online issue, which is available at wileyonlinelibrary.com.]

Mannich base and phenolic structure (see "Thermal Stability of Cured 1 and 2 Under Nitrogen" for details).

The apparent activation energy ($E_a$) of the curing reaction of precursors **1** and **2** can be calculated by using well-known Kissinger's and Ozawa's method.[56] Kissinger's method assumes that $T_p$ varies with the heating rate and the maximum reaction rate occurs at $T_p$. According to Kissinger's equation:

$$\frac{d\left[\ln\left(\beta/T_p^2\right)\right]}{d\left(1/T_p\right)} = -\frac{E_a}{R} \quad (1)$$

where $\beta$ is the heating rate, $T_p$ is the exothermic peak temperature, $A$ is the pre-exponential factor, $E_a$ is the apparent activation energy, and $R$ is the universal gas constant, plots of

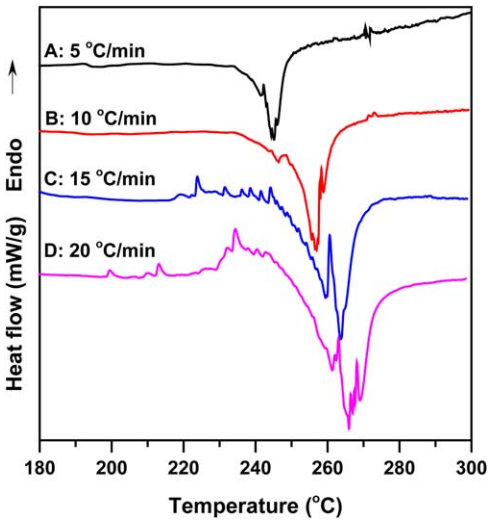


**Figure 7.** Nonisothermal DSC curves for *m*-carborane bisphenol benzoxazine precursor (**2**) at (A) 5, (B) 10, (C) 15, and (D) 20 °C/min. [Color figure can be viewed in the online issue, which is available at wileyonlinelibrary.com.]

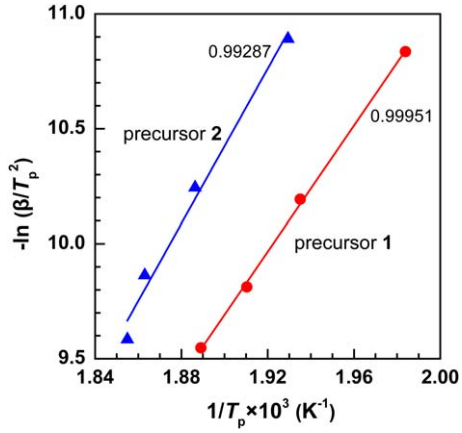


**Figure 8.** Plots of $\ln\left(\beta/T_p^2\right)$ as a function of $1/T_p$ for precursors **1** and **2** to calculate $E_a$ according to Kissinger's method. [Color figure can be viewed in the online issue, which is available at wileyonlinelibrary.com.]

$\ln\left(\beta/T_p^2\right)$ against $1/T_p$ are prepared and shown as straight lines in Figure 8. The Pearson's linear correlation coefficient was calculated and given near the line.

Ozawa's method assumes that the degree of conversion at peak temperatures for different heating rates is constant. According to Ozawa's equation:

$$\ln\beta = -1.052\frac{E_a}{RTp} + C \quad (2)$$

where $C$ is constant, plots of $\ln\beta$ against $1/T_p$ are prepared and shown as a straight line in Figure 9.

The apparent activation energies ($E_a$) of the curing reaction of precursors **1** and **2** were calculated from the slope of lines in Figures 7 and 8 and summarized in Table III. Precursor **1** owns lower $E_a$, indicating that precursor **1** is easier to be cured than precursor **2**. The electron-withdrawing ability of carbons on *o*-carborane cage is higher than those on *m*-carborane, thus *o*-carborane-containing precursor **1** exhibits higher reactivity than its

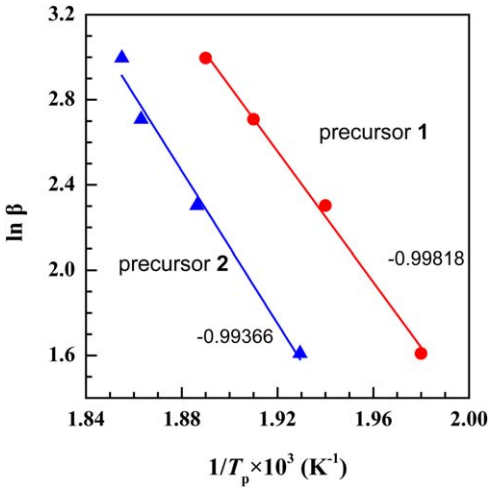


**Figure 9.** Plots of $\ln\beta$ as a function of $1/T_p$ for precursors **1** and **2** to calculate $E_a$ according to Ozawa's method. [Color figure can be viewed in the online issue, which is available at wileyonlinelibrary.com.]

**Table III.** $E_a$ Values Obtained from Nonisothermal Data

| Precursor | $E_a$/kJ mol$^{-1}$ | |
|---|---|---|
| | Kissinger's method | Ozawa's method |
| **1** | 113.95 | 121.11 |
| **2** | 139.95 | 141.38 |

*meta* counterpart. On the other hand, very close $E_a$ values were obtained through different methods, which verified the nonisothermal DSC studies of the curing kinetics of benzoxazine precursors.

The optimum curing temperatures could be determined from the characteristic temperatures at a heating rate of 0 °C/min, $T_{i0}$, $T_{p0}$, and $T_{t0}$, which were obtained by the extrapolation of the plots of characteristic temperatures, $T_i$, $T_p$, and $T_t$, as a function of heating rates ($\beta$). Figure 10 shows the plots for the curing behavior of precursor **1** and the characteristic temperatures at a heating rate of 0 °C/min were shown in Table IV.

The optimum curing processes of precursors **1** and **2** were determined according to Table IV. **1** was cured at 200 °C for 2 h and then at 220 °C for 2 h, while **2** was cured at 150 °C for 2 h and then at 240 °C for 2 h. Both precursors were fully cured under the above curing conditions. The FTIR spectrum of cured **2** is shown in Figure 2(C). Compared with the FTIR spectrum of precursor **2**, the absorption peaks at 1034 and 1228 cm$^{-1}$ associated with the symmetric and asymmetric vibrations of C—O—C and 1162 and 1385 cm$^{-1}$ ascribed to the symmetric and asymmetric vibrations of C—N—C disappeared from the spectrum of cured **2**, indicating that the benzoxazine rings were completely consumed during the curing process. Besides, new absorption peak at 3356 cm$^{-1}$ appeared which was assigned to the stretching vibration of phenolic hydroxyl group formed through oxazine ring-opening reaction.

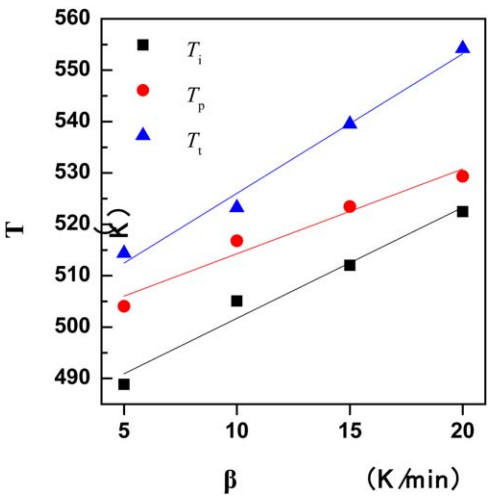


**Figure 10.** Plots of characteristic temperatures ($T_i$, $T_p$, and $T_t$) as a function of heating rate ($\beta$) for the curing behavior of precursor **1**. [Color figure can be viewed in the online issue, which is available at wileyonlinelibrary.com.]

**Table IV.** Characteristic Temperatures at a Heating Rate of 0 °C/min for the Curing Behavior of Precursor 1 and 2

| | $\beta$/°C min$^{-1}$ | $T_i$/°C | $T_p$/°C | $T_t$/°C | $T_{i0}$/°C | $T_{p0}$/°C | $T_{t0}$/°C |
|---|---|---|---|---|---|---|---|
| **1** | 5 | 215.7 | 230.9 | 241.2 | 207.0 | 224.6 | 225.7 |
| | 10 | 231.9 | 243.6 | 250.1 | | | |
| | 15 | 238.9 | 250.3 | 266.4 | | | |
| | 20 | 249.3 | 256.2 | 281.0 | | | |
| **2** | 5 | 175.8 | 245.2 | 256.7 | 148.0 | 240.7 | 243.0 |
| | 10 | 178.9 | 257.0 | 271.0 | | | |
| | 15 | 244.3 | 263.6 | 287.6 | | | |
| | 20 | 234.6 | 265.9 | 298.4 | | | |

### Thermal Stability of Cured 1 and 2 under Nitrogen

Carborane-containing polymers are well-known for their ultrahigh char yield at elevated temperatures.[17] Therefore, it is of great significance to study the thermal stability of carborane bisphenol-based benzoxazine resins (cured **1** and **2**). Thermal gravimetric analysis (TGA) technique was utilized and the recorded TGA thermograms of cured **1** and **2** under nitrogen are shown in Figure 11. The TGA curve of a typical bisphenol A-based benzoxazine resin (BA-a) is also given for comparison. The decomposition temperature ($T_d$) is defined as the temperature at which the resin loses 5% of its original weight. Thus, the $T_d$ values for cured **1** and **2** are picked up from the TGA curves as 347 and 354 °C, higher than the $T_d$ of BA-a (319 °C). The limited improvement of decomposition temperature can be ascribed to the shielding effect of carborane cages incorporated into the benzoxazine resins. It is also seen from Figure 10 that carborane-containing benzoxazine resins (cured **1** and **2**) own much higher char yield at 900 °C (76.8% for cured **1** and 72.6% for cured **2**) than carborane-free resin (BA-a, 33.1%). To the best of our knowledge, carborane bisphenol-based benzoxazine resins studied in this work seem to own the highest char yield among their family. It is believed that the existence of carborane

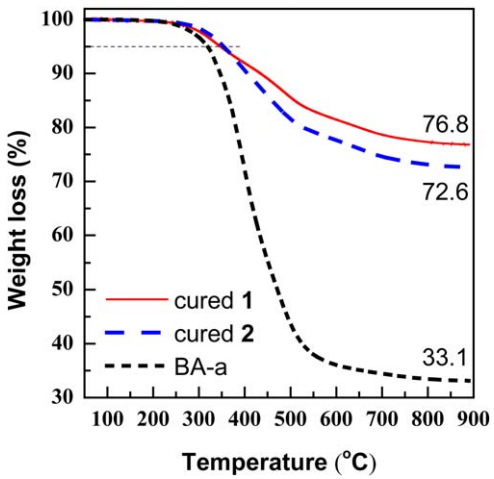


**Figure 11.** TGA curves of cured **1** and **2** under nitrogen. TGA curve of BA-a is also given for comparison. [Color figure can be viewed in the online issue, which is available at wileyonlinelibrary.com.]

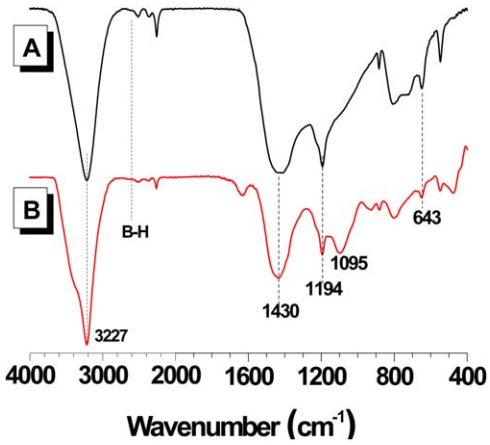


**Figure 12.** FTIR spectra of *m*-carborane bisphenol benzoxazine resin (cured **2**) after TGA test under (A) nitrogen and (B) air. [Color figure can be viewed in the online issue, which is available at wileyonlinelibrary.com.]

cages contributes to the thermal stability of carborane-containing benzoxazine resins.

FTIR spectroscopy was utilized to study the structural variation of carborane bisphenol-based benzoxazine resins and the FTIR spectrum of cured **2** after TGA test under nitrogen was shown in Figure 12(A). The disappearance of stretching vibration peak at 2600 $cm^{-1}$ indicates complete consumption of B—H bonds on carborane cage at elevated temperature. Besides, fine absorption peaks below 1700 $cm^{-1}$ disappear, accounting for the destruction of organic fragments of the benzoxazine resin. Absorption peaks around 1430, 1194, and 643 $cm^{-1}$ are ascribed to the stretching vibrations of B—O—B, B—OH, and B—C respectively. It is concluded from the above analysis that a three-dimensional polymer network is compacted by forming B—O—B and B—C linkages, just as the case of carborane-containing phenolic resin.[57] The organic fragments decompose into radicals at elevated temperature. However, the formed radicals cannot move freely through the above thermally stable network, and thus fail to undergo secondary recombination processes. In this way, the boron-rich network successfully inhibits further polymer degradation processes.

DTG curve analysis provides more information on the degradation process at high temperatures. Figure 13 shows the weight loss rates of BA-a, cured **1**, and cured **2**. It can be seen that BA-a exhibits a trimodal derivative curve with a maximum rate of 0.43%/°C at 398 °C. The peak overlap is due to the fact that both Mannich base and phenolic structure degrade simultaneously with different onset temperatures, according to Ishida's work.[58] The weight loss rates of cured **1** and **2** (below 0.1%/°C) are much lower than that of BA-a, indicating the hindrance of carborane structure on the degradation of benzoxazine resins. The DTG curve of cured **2** also shows a maximum derivative peak at 398 °C, which is the synergistic result of Mannich base breakdown and phenolic structure degradation. For cured **1**, we expected to obtained similar derivative curve as cured **2**, but are surprised to find that there exists a valley around 403 °C. Considering the simultaneous degradation of Mannich base and phenolic structure around 398 °C, there is supposed to be a maximum peak due to the overlap. However, the cage isomerization shift from *o*-carborane to *m*-carborane occurs in the same temperature range (~450 °C), which absorbs energy and blocks the anticipated degradation.[59] Therefore, the two peaks fail to overlap with each other, which contributes to the assignment of each peak. The first peak at 337 °C is assigned to the Mannich base degradation, while the second peak at 489 °C is assigned to phenolic structure decomposition. The above peak separation phenomenon was also observed in the DTG studies of *p*-cresol- and 2,2′-bisphenol-based benzoxazine resins.[58] Different from BA-a, the DTG curve of cured **1** and **2** appear noticeable degradation tails at temperatures higher than 600 °C because carborane cages continue their reactions with phenolic hydroxyl and atmospheric moisture to form the above boron-rich network.

### Thermo-oxidative Stability of Cured 1 and 2 under Air

To study the thermal oxidation of carborane bisphenol-based benzoxazine resins, TGA and DTG analyses of cured **1** and **2** were further conducted under air and the results are shown in Figures 14 and 15. Bisphenol A-based benzoxazine resin (BA-a) was also studied under the same conditions for comparison. It is seen that $T_d$ values for cured **1** and **2** are 412 and 359 °C respectively, much higher than the $T_d$ of BA-a (261 °C), indicating that the existence of carborane moiety also postponed the initial oxidative degradation of benzoxazine resins by virtue of its shielding effect on the adjacent organic fragments.

Further thermo-oxidation of BA-a followed a two-stage process. At the first stage, the weight loss proceeded at a moderate rate of 0.15–0.20%/°C from 250 to 500 °C, which was attributed to the simultaneous decomposition of organic fragments, i.e., Mannich base and phenolic moiety. At the second stage, BA-a lost almost all its weight up to 700 °C with the highest weight loss rate of 0.64%/°C at 631 °C, corresponding to the thermo-oxidation of the formed char into carbon dioxide.[58] Owing to the existence of carborane moiety, the weight loss of carborane bisphenol-based benzoxazine resins (cured **1** and **2**) proceeded in quite different ways. For cured **2**, there only exists one

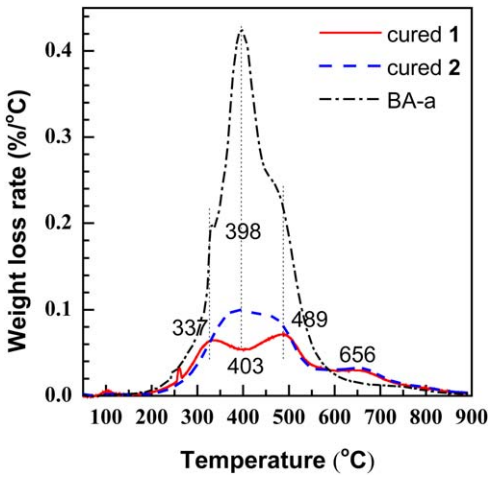


**Figure 13.** DTG curves of cured **1** and **2** under nitrogen. DTG curve of BA-a is also given for comparison. [Color figure can be viewed in the online issue, which is available at wileyonlinelibrary.com.]

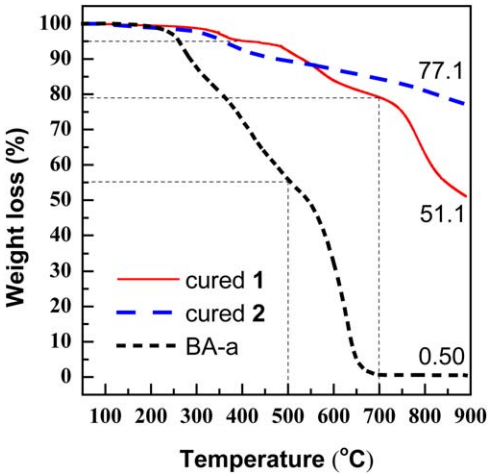


**Figure 14.** TGA curves of cured **1** and **2** under air. TGA curve of BA-a is also given for comparison. [Color figure can be viewed in the online issue, which is available at wileyonlinelibrary.com.]

noticeable thermo-oxidation peak around 361 °C with the weight loss rate of 0.06%/ °C ascribed to the decomposition of organic fragments (Figure 15), while no drastic weight loss of cured **2** appeared at higher temperature. Due to the participation of oxygen, the char was formed as three-dimensional polymer network with more B—O—B linkages at elevated temperature [Figure 12(B)], and thus failed to undergo further thermo-oxidation and give rise to major weight loss.

As for cured **1**, it is obvious from Figure 14 that the thermo-oxidation process consists of three stages. The first stage coincidently fell in the temperature range of 250–450 °C where cured **2** appeared its maximum weight loss rate, and thus could be assigned to the oxidative degradation of organic fragments. To explore the origin of last two stages, a char material from the degradation of cured **1** under nitrogen was further degraded under air, and the results were shown in Figure 16. It is obvious that the char material undergoes two major weight losses in the

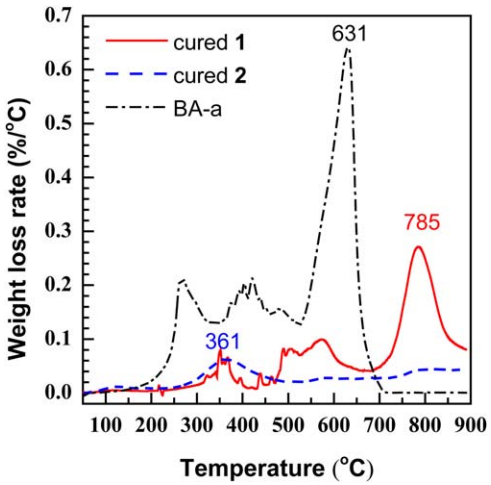


**Figure 15.** DTG curves of cured **1** and **2** under air. DTG curve of BA-a is also given for comparison. [Color figure can be viewed in the online issue, which is available at wileyonlinelibrary.com.]

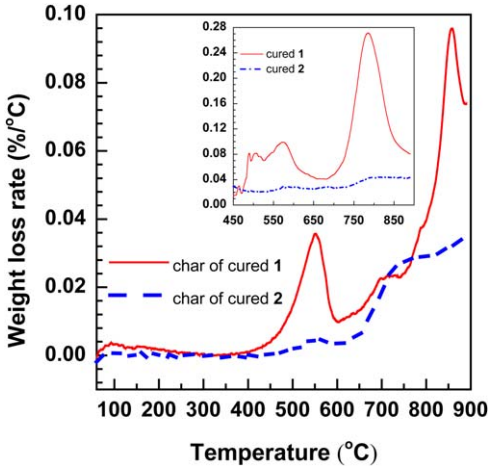


**Figure 16.** DTG curves of the formed chars of cured **1** and **2** under air. Chars were obtained by degrading cured **1** and **2** under nitrogen. Inserted are DTG curves of cured **1** and **2** under air at elevated temperature. [Color figure can be viewed in the online issue, which is available at wileyonlinelibrary.com.]

temperature range of 450–900 °C, which is in approximate agreement with the weight loss of cured **1** in the same temperature range under air. Therefore, the weight loss of cured **1** under air at temperatures higher than 450 °C is attributed to the thermo-oxidation of the formed char. We assume that *o*-carborane moiety owns poorer asymmetry than its meta- counterpart, which causes uneven distribution of boron in the formed char. Consequently, the formed char from cured **1** could be partly degraded.

At the same time, the degradation of the char from cured **2** was also studied and the result again verified the fact that no major thermo-oxidation of cured **2** occurred at higher temperature.

## CONCLUSIONS

In summary, two carborane-containing benzoxazine precursors (**1** and **2**) were successfully synthesized in higher yields by the Mannich reaction of corresponding carborane bisphenol (**3** and **4**) with anline and formaldehyde in 1,4-dioxane. The obtained precursors showed satisfactory ring content and their structures have been well characterized with spectroscopic characterization techniques including GPC, FTIR, $^{1}$H NMR, $^{13}$C NMR, and $^{11}$B NMR. The curing behaviors of precursors **1** and **2** were studied by nonisothermal DSC tests. Kissinger's and Ozawa's methods were utilized to calculate the apparent activation energies ($E_a$) of the curing reactions, and the results showed approximately 120 kJ mol$^{-1}$ for precursor **1** and 140 kJ mol$^{-1}$ for precursor **2**, indicating that **1** is easier to be cured than **2** owing to higher electron-withdrawing ability of carbons on *o*-carborane cage. Besides, the plots of characteristic temperatures from DSC data were extrapolated to give the optimum curing processes, 200 °C/2 h + 220 °C/2 h for **1** and 150 °C/2 h + 240 °C/2 h for **2**, under which both precursors were fully cured to obtain benzoxazine resins.

TGA analyses manifested that the incorporation of carborane moiety endowed the obtained benzoxazine resins (cured **1** and

**2**) with excellent thermal stability and unique thermo-oxidative stability. $T_d$ values for cured **1** and **2** under nitrogen were 347 and 354 °C, respectively, higher than $T_d$ of BA-a (319 °C). While under air these values became 412 and 359 °C, also much higher than the $T_d$ of BA-a (261 °C). The above results showed that the initial degradation of both cured **1** and **2** under nitrogen and air was postponed to some extent owing to the shielding effect of carborane moiety on adjacent organic fragments. At higher temperature three-dimensional polymer networks with B-O—B and B–C linkages were formed as chars by the reaction of carborane cage with atmospheric moisture, degradation products such as phenolic hydroxyl, and oxygen (under air). Under nitrogen this network hindered the motion of radicals formed at elevated temperature and thus inhibited further polymer degradation processes. Therefore, both cured **1** and **2** owned ultrahigh char yields (76.8 and 72.6% at 900 °C) under inert atmosphere. While under air, the formed boron-rich networks could hardly be further oxidized into carbon dioxide so that the carborane-containing benzoxazine resins also showed very high char yields (51.1% for cured **1** and 77.1% for cured **2** at 900 °C) under oxidative environment. It should be noted that cured **1** underwent partial char degradation beyond 450 °C due to uneven distribution of boron in the formed char, while the char of cured **2** could hardly be degraded even at temperature up to 900 °C.

## ACKNOWLEDGMENTS

The authors would like to acknowledge the financial support from the Fundamental Research Funds for the Central Universities (JD-1512).

## REFERENCES

1. Sawaryn, C.; Kreiling, S.; Schonfeld, R.; Landfester, K.; Taden, A. In Handbook of Benzoxazine Resins; Ishida, H.; Hatsuo, I; Tarek, A., Eds.; Elsevier: Amsterdam, **2011**; Chapter 35, p 605.
2. Kumar, K. S. S.; Nair, C. P. R. In Polybenzoxazines: Chemistry and Properties; iSmithers: Shrewsbury, **2010**; Chapter 4, p 131.
3. Nair, C. P. R. *Prog. Polym. Sci.* **2004**, *29*, 401.
4. Chernykh, A.; Agag, T.; Ishida, H. *Polymer* **2009**, *50*, 3153.
5. Kim, H. J.; Brunovska, Z.; Ishida, H. *J. Appl. Polym. Sci.* **1999**, *73*, 857.
6. Kumar, K. S. S.; Nair, C. P. R.; Radhakrishnan, T. S.; Ninan, K. N. *Eur. Polym. J* **2007**, *43*, 2504.
7. Agag, T.; Takeichi, T. *Macromolecules* **2003**, *36*, 6010.
8. Cao, G. P.; Chen, W. J.; Liu, X. B. *Polym. Degrad. Stab.* **2008**, *93*, 739.
9. Liu, Y.; Zhao, S.; Zhang, H.; Wang, M.; Run, M. *Thermochim. Acta* **2012**, *549*, 42.
10. Liu, Y. L.; Yu, J. M.; Chou, C. I. *J. Polym. Sci. A: Polym. Chem.* **2004**, *42*, 5954.
11. Ishida, H.; Ohba, S. *Polymer* **2005**, *46*, 5588.
12. Liu, Y. L.; Chou, C. I. *J. Polym. Sci. A: Polym. Chem.* **2005**, *43*, 5267.
13. Chang, H. C.; Lin, H.; Tian, Y. W.; Feng, Y. R.; Chan, L. H. *J. Polym. Sci. A: Polym. Chem.* **2012**, *50*, 2201.
14. Lu, Y.; Li, M.; Zhang, Y.; Hu, D.; Ke, L.; Xu, W. *Thermochim. Acta* **2011**, *515*, 32.
15. Su, Y. C.; Chen, W. C.; Chang, F. C. *J. Appl. Polym. Sci* **2004**, *94*, 932.
16. Shen, S. B.; Ishida, H. *J. Appl. Polym. Sci.* **1996**, *61*, 1595.
17. Grimes, R. N. Carboranes, 2nd ed.; Elsevier: New York, **2011**; Chapter 9, p 301, Chapter 10, p 541.
18. Peters, E. N. *Indus. Eng. Chem. Prod. Res. Dev.* **1984**, *23*, 28.
19. Henderson, L. J.; Keller, T. M. *Macromolecules* **1994**, *27*, 1660.
20. Sundar, R.; Keller, T. M. *J. Polym. Sci. A: Polym. Chem.* **1997**, *35*, 2387.
21. Izmailov, B. A.; Nedelkin, V. I.; Gerr, I. S. *Russ. Chem. Bull.* **1998**, *47*, 687.
22. Patel, M.; Swain, A. C.; Skinner, A. R.; Mallinson, L. G.; Hayes, G. F. *Macromol. Symp.* **2003**, *202*, 47.
23. Patel, M.; Swain, A. C. *Polym. Degrad. Stab.* **2004**, *83*, 539.
24. Patel, M.; Swain, A. C.; Cunningham, J. L.; Maxwell, R. S.; Chinn, S. C. *Polym. Degrad. Stab.* **2006**, *91*, 548.
25. Zhang, X.; Kong, L.; Dai, L.; Zhang, X.; Wang, Q.; Tan, Y.; Zhang, Z. *Polymer* **2011**, *52*, 4777.
26. Jiang, Y.; Lv, Y.; Li, Y. *Polym. Mater. Sci. Eng.* **2014**, *30*, 1.
27. Men, X.; Cheng, Y.; Chen, G.; Bao, J.; Yang, J. *High Perform. Polym.* **2014**; published online. DOI: 10.1177/0954008314557049.
28. Qi, S.; Wang, Y.; Han, G.; Yang, Z.; Zhang, X.; Jiang, S.; Lv, Y. *Acta Polym. Sin.* **2015**, *8*, 921.
29. Abramova, T. M.; Alekseyeva, S. G.; Valetskii, P. M.; Golubenkova, L. I.; Makarova, I. M.; Slonim, I. Y.; Urman, Y. G.; Shabadash, A. N. *Vysokomol Soyed* **1980**, *22*, 1637.
30. Qi, S.; Han, G.; Wang, H.; Li, N.; Zhang, X. A.; Jiang, S.; Lu, Y. *Chinese J. Polym. Sci.* **2015**, *33*, 1606.
31. Vinogradova, S. V.; Valetskii, P. M.; Kabachii, Y. A. *Russ. Chem. Rev.* **1995**, *64*, 365.
32. Galie, K. M.; Mollard, A.; Zharov, I. *Inorg. Chem.* **2006**, *45*, 7815.
33. Parrott, M. C.; Valliant, J. F.; Adronov, A. *Langmuir* **2006**, *22*, 5251.
34. Benhabbour, S. R.; Parrott, M. C.; Gratton, S. E. A.; Adronov, A. *Macromolecules* **2007**, *40*, 5678.
35. Kolel-Veetil, M. K.; Dominguez, D. D.; Keller, T. M. *J. Polym. Sci. A: Polym. Chem.* **2008**, *46*, 2581.
36. Djeda, R.; Ruiz, J.; Astruc, D.; Satapathy, R.; Dash, B. P.; Hosmane, N. S. *Inorg. Chem.* **2010**, *49*, 10702.
37. Dash, B. P.; Satapathy, R.; Bode, B. P.; Reidl, C. T.; Sawicki, J. W.; Mason, A. J.; Mason, J. A.; Hosmane, N. S. *Organometallics* **2012**, *31*, 2931.
38. Li, N.; Zhao, P.; Salmon, L.; Ruiz, J.; Zabawa, M.; Hosmane, N. S.; Astruc, D. *Inorg. Chem.* **2013**, *52*, 11146.

39. Peterson, J. J.; Were, M.; Simon, Y. C.; Coughlin, E. B.; Carter, K. R. *Macromolecules* **2009**, *42*, 8594.
40. Kokado, K.; Chujo, Y. *Macromolecules* **2009**, *42*, 1418.
41. Kokado, K.; Tominaga, M.; Chujo, Y. *Macromol. Rapid Commun.* **2010**, *31*, 1389.
42. Kokado, K.; Nagai, A.; Chujo, Y. *Macromolecules* **2010**, *43*, 6463.
43. Peterson, J. J.; Davis, A. R.; Were, M.; Coughlin, E. B.; Carter, K. R. *ACS Appl. Mater. Interfaces* **2011**, *3*, 1796.
44. Davis, A. R.; Peterson, J. J.; Carter, K. R. *ACS Macro Lett.* **2012**, *1*, 469.
45. Ishida, H.; Rodriguez, H. *Polymer* **1995**, *36*, 3151.
46. Kim, H.; Ishida, H. *J. Phys. Chem. A* **2002**, *106*, 3271.
47. Kimura, H.; Matsumoto, A.; Hasegawa, K.; Ohtsuka, K.; Fukuda, A. *J. Appl. Polym. Sci.* **1998**, *68*, 1903.
48. Liu, Y.; Wang, M.; Zhang, H.; Zhao, S.; Run, M. *Polym. Adv. Technol.* **2013**, *24*, 157.
49. Agag, T.; Jin, L.; Ishida, H. *Polymer* **2009**, *50*, 5940.
50. Wang, J.; Fang, X.; Wu, M.; He, X.; Liu, W.; Shen, X. *Eur. Polym. J.* **2011**, *47*, 2158.
51. Fu, Z.; Liu, H.; Cai, H.; Liu, X.; Ying, G.; Xu, K.; Chen, M. *Polym. Eng. Sci.* **2012**, *52*, 2473.
52. Lu, Y.; Li, M.; Ke, L.; Hu, D.; Xu, W. *J. Appl. Polym. Sci.* **2011**, *121*, 2481.
53. Huang, X.; Zhang, Q.; Meng, Z.; Gu, J.; Jia, X.; Xi, K. *J. Polym. Sci. A: Polym. Chem.* **2015**, *53*, 973.
54. Ning, X.; Ishida, H. *J. Polym. Sci. A: Polym. Chem.* **1994**, *32*, 1121.
55. Causey, P. W.; Besanger, T. R.; Valliant, J. F. *J. Med. Chem.* **2008**, *51*, 2833.
56. Jubsilp, C.; Punson, K.; Takeichi, T.; Rimdusit, S. *Polym. Degrad. Stab.* **2010**, *95*, 918.
57. Bekasova, N. I. *Russ. Chem. Rev.* **1984**, *53*, 61.
58. Low, H. Y.; Ishida, H. *Polymer* **1999**, *40*, 4365.
59. Johnson, B. F. G.; Roberts, Y. V.; Parisini, E. *Inorg. Chim. Acta* **1993**, *211*, 17.